

We are IntechOpen, the world's leading publisher of Open Access books Built by scientists, for scientists

6,900

Open access books available

186,000

International authors and editors

200M

Downloads

Our authors are among the

154

Countries delivered to

TOP 1%

most cited scientists

12.2%

Contributors from top 500 universities



WEB OF SCIENCE™

Selection of our books indexed in the Book Citation Index
in Web of Science™ Core Collection (BKCI)

Interested in publishing with us?
Contact book.department@intechopen.com

Numbers displayed above are based on latest data collected.
For more information visit www.intechopen.com



Terahertz Spectroscopy for Gastrointestinal Cancer Diagnosis

Faustino Wahaia, Irmantas Kašalynas,
Gintaras Valušis, Catia D. Carvalho Silva and
Pedro L. Granja

Additional information is available at the end of the chapter

<http://dx.doi.org/10.5772/66999>

Abstract

In this chapter, we present a number of sensitive measurement modalities for the study and analysis of human cancer-affected colon and gastric tissue using terahertz (THz) spectroscopy. Considerable advancements have been reached in characterization of bio-tissue with some accuracy, although too dawn, and still long and exhaustive work have to be done towards well-established and reliable applications. The advent of the THz-time-domain spectroscopy (THz-TDS) test modality at a sub-picosecond time resolution has arguably fostered an intensive work in this field's research line. The chapter addresses some basic theoretical aspects of this measurement modality with the presentation of general experimental laboratory setup diagrams for THz generation and detection, sample preparation aspects, samples optical parameters calculation procedures and data analysis.

Keywords: spectroscopy, absorption, ATR mode, reflection and transmission, carcinomas

1. Introduction

Terahertz (THz) (10^{12} Hz) frequency band is a small section of the electromagnetic spectrum lying between the microwave and infrared (IR) regions sometimes referred to as THz gap or T-rays. There is no standard definition for the THz band, but it has most often come to refer to frequencies in the range of 0.1–10 THz [1–3]. The results of several studies [4–7] using terahertz techniques started the breakneck race of even more studies towards biomedical applications of terahertz technology.

1.1. Terahertz technology advantages

The energies of THz radiation are significantly lower such that at 1 THz, the energy is about 4.1 meV [8]; compared to X-rays (with photon energy typically in order of few keV [9], i.e., few million times higher than that for THz photon energy), it is considered non-ionizing. In the absorption processes where THz waves interact with biological media, the Gibbs free energy conveyed in the THz photons beam is not sufficient to induce any chemical reactions [10]; therefore, any measurement technique operating at this frequency range and at reasonably low power levels could be considered as non-invasive and offers higher contrast spectral features; almost all dielectric materials are transparent to THz radiation; it gives an unambiguous information concerning big molecules; it offers higher spatial resolution compared to infrared one, therefore much better for imaging purposes; meanwhile, IR frequency band brings only local information on molecules, gives only information on chemical binding between shortest neighbours, and THz radiation brings global information on molecules, gives information on the whole molecule and its specific rotation-vibrational modes [11]. So that the frequency band could be of paramount importance for the study and characterization of biological media.

The vibrational spectral fingerprint of biomolecules lies in this frequency range [12, 13] (and many materials of interest have unique spectral fingerprints in the terahertz range [14, 15]), therefore, it can be used for their identification, making THz spectroscopy a promising sensing tool for biomedical applications and disease diagnosis.

Due to space constraints, we avoided, in the present chapter, broad practical considerations on methods, and by the nowadays, vast applications of THz spectroscopy. Being confident in having counted with the contribution of leading experts in the field of THz technology, we realize that the chapter will be concise and comprehensive. We aim at providing a representative overview of the current state of art of THz spectroscopy for cancer detection, as well as for colon and stomach cancer particularly.

The development of ultrafast lasers and the discovery of the Auston switch in the 1970s [16] led to a new generation of THz spectrometers in the early 1990s [17] that were able to generate and detect pulses of coherent terahertz radiation with unprecedented ease and sensitivity. The generation and detection diagram are presented in **Figure 1**.

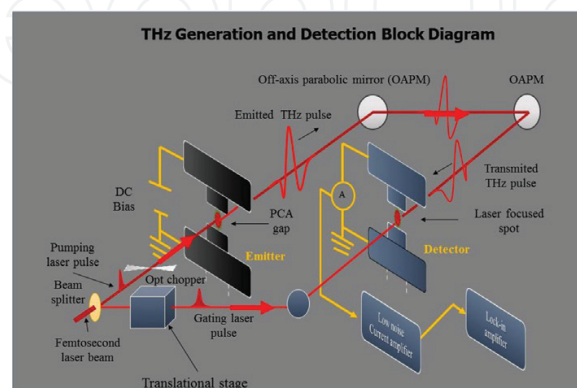


Figure 1. Diagram of THz generation and detection. The emitter is on the left; the receiver is on the right. The THz pulse is recorded as a function of time delay and the obtained time-domain signal is Fourier-transformed numerically.

2. Terahertz time-domain spectroscopy

Since 1990s, the research towards the application of THz spectroscopy to probe and characterize various biomolecules has advanced considerably. The THz time-domain spectroscopy (THz-TDS) is actually a spectroscopic technique in which the properties of a material are investigated using THz short pulses. Their generation and detection scheme is sensitive to the material's effect on both the amplitude and the phase. The technique can provide more information than conventional Fourier-transform spectroscopy (FTS), which is only sensitive to the amplitude. Therefore, it could be a useful analytical tool for materials study and characterization.

An ultrashort optical pulse (normally femtosecond [fs] in duration) is used to pump (illuminate) a photoconductive (PC) semiconductor creating pairs of photocarriers (electron-hole pairs). The photoconductive (PC) material changes suddenly from being an insulator into being a conductor. Then the conduction state leads to an abrupt electrical current across a biased kind of dipole antenna stuck on a semiconductor substrate referred to as photoconductive antenna (PCA). This changing current emits short pulse (~2 picoseconds [ps]) [18] THz electromagnetic field.

Typically, there are two electrodes stuck on a low temperature grown gallium arsenide (LTG-GaAs), semi-insulating gallium arsenide (SiGaAs), indium phosphate (InP) substrate or other semiconductor material. The electrodes are made in the form of a simple dipole antenna with a gap (G) of a few microns (~5 μm) and have a bias voltage up to 40 V between them (Figure 2).

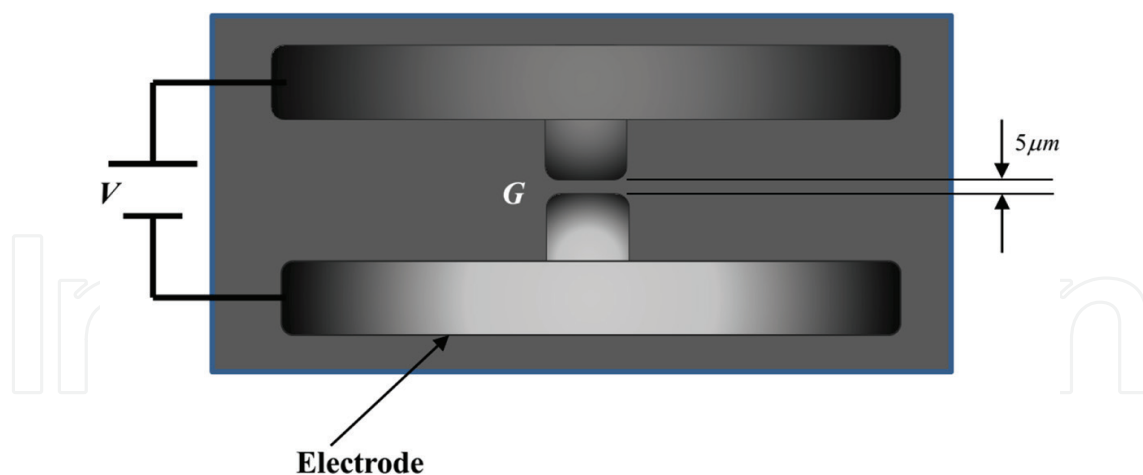


Figure 2. Diagram of a PCA for THz emission and detection.

And, the other one is the probe pulse, and goes through a translational stage to provide a relative periodical time delay [19] (typically controlled by changing the relative path between the pump and probe beams with a linear stage). Both the pump and probe pulses are derived from the same optical beam and, therefore, have the same duration, which typically has a range between 10 and 150 fs. Usually, another PCA is used as detector, which,

interacting with the probe, generates an electrical signal proportional to the amplitude of the THz pulse for that particular time delay, that is, it samples the THz signal in the detector. There are other methods besides that based on photoconductive antennas, such as based on optical rectification, wherein, by passing high-intensity femtosecond laser pulses through a transparent crystal such as zinc telluride (ZnTe), gallium phosphide (GaP), and gallium selenide (GaSe), a terahertz short pulse is generated in this case biasing is not needed. The process is nonlinear where anyone of above mentioned crystals is suddenly electrically polarized at high laser intensities (amplified). The so changing electrical polarization emits terahertz radiation.

The detection process is similar with that for generation (PC detection). To do that, the bias electrical field across the detecting PCA is generated by the THz electric field pulses this time. The THz electric field generates current across the receiving PCA connections wires. A low-noise amplifier is used for the signal amplification. And, finally, the amplified current is the measured parameter, which is proportional to the THz field transient. A lock-in amplifier (LIA) is also used to demodulate the signal, and this avoids $1/f$ (flicker) noise problems that are present in the detector-limited measurement scheme.

The THz signal is directly measured as a function of time, and the frequency spectra of both sample material signal and reference (without sample) one are obtained by a numerical Fourier transformation. Further calculations of the obtained spectra yield the spectroscopic information of the sample material under study. Since the measurements are made on electric field instead of intensity, both amplitude and phase can be determined at once, thus leading to the calculation of the sample's frequency-dependent optical constants such as absorption coefficient and the refractive index. This is an advantage compared to the well-established Fourier transform spectroscopy (FTS), which is based on the intensity detection with recourse to Kramers-Kronig [20] data treatment, with all the uncertainties associated.

Terahertz spectroscopy for cancer detection is arguably among the most active research topics within the research groups in the field of T-rays' technology. The utmost importance of the information obtained by THz spectroscopic technique has incentivized the researchers to keep seeking for efficient source and sensitive detectors. As was stated previously, this chapter will not provide a full review of the works performed in this field. It otherwise intends to show (on the base of selected few previous works) the potential of this technique for gastrointestinal (GI) cancer detection particularly.

A THz-TDS is a pump-probe-like technique [21] since the signal and reference are measured by sampling using a delayed probe optical pulse, taking the form of a time trace with sub-picosecond resolution. The signal-to-noise ratio (SNR) is much higher than that of Fourier transform infrared spectroscopy (FTIR) [22]. The Coherent-gated detection gives a noise equivalent power of $\sim 10^{-16}$ W/ $\sqrt{\text{Hz}}$, which is six orders of magnitude better than the pyro-detectors, normally used in Fourier transform spectrometers. A typical setup diagram for THz-TDS measurements is shown in **Figure 3**.

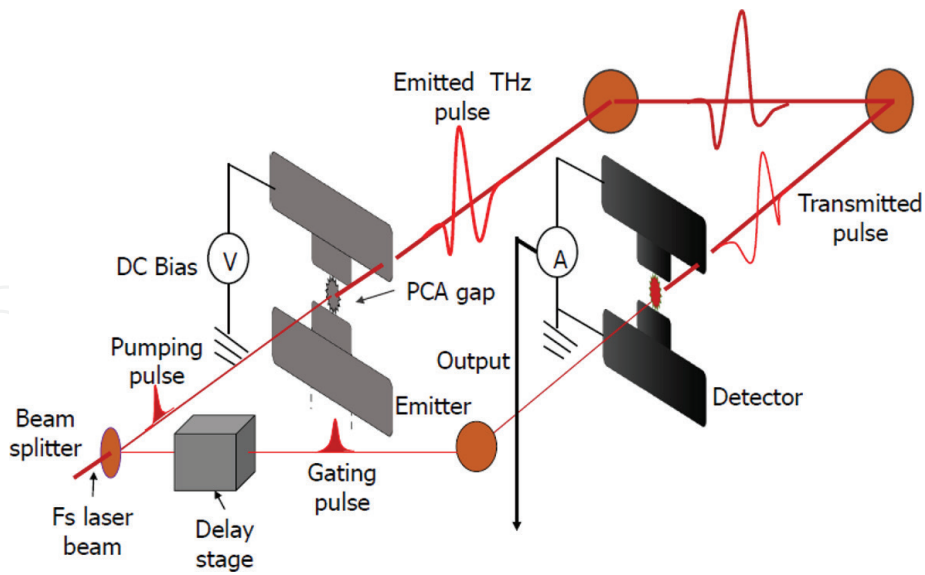


Figure 3. Typical experimental setup for THz spectrometer using photoconductive antennas (PCAs) in the transceiver.

3. Time-domain terahertz spectroscopy in reflection geometry

In this modality, the measurements can be performed by reflection geometry (**Figure 4**) as well as by attenuated total reflection (ATR) [23–25]; the use of an evanescent wave (i.e., a THz wave illuminates the interface of two media, with different refractive indices n_1 and n_2 , at a certain critical angle θ_c and the wave is totally reflected at the interface). Then, part of the wave enters and propagates through the studied medium at a short distance (known as evanescent wave). This method is required in measurements involving strongly absorbing materials and in transmission geometry involving no or slightly absorbing ones.

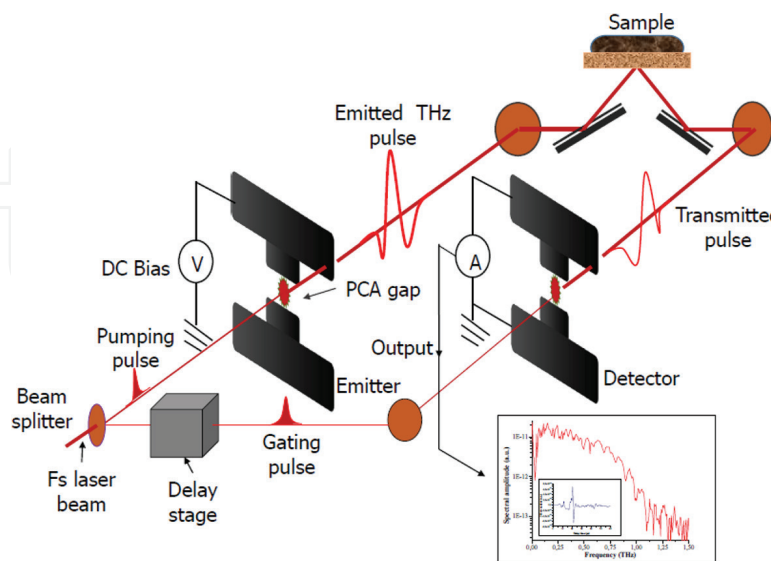


Figure 4. General experimental setup for THz-TDS in reflection geometry. The sample (colon or gastric tissue) is sandwiched in between two high density polyethylene (HDPE) or other window material sheets, normally.

As the THz signal is extremely weak in the order of $>10 \mu\text{W}$ [26], an lock-in amplifier (LIA) is used to extract the signal from the thermal background. Due to the coherent and gated detection nature of the THz-TDS technique, the signals are almost unmasked by the thermal background noise. A computer controls the delay line, reads the LIA values at each position and records the THz pulse waveforms. The amplitude and phase information of the THz field, as foretold, are accounted at once [27]. The THz properties of samples are measured with the difference between the generated THz pulse, E_{ref} and the transmitted sample THz pulse, E_s : using Fast Fourier Transform, these signals provide complex-valued optical properties such as refractive indices, absorption coefficients, dielectric constants and conductivities.

The technique provides more information if compared with a conventional Fourier-transform spectroscopy (FTS), which is only sensitive to the amplitude. THz radiation has several distinct advantages over other forms of spectroscopy: Examples which have been demonstrated include several different types of explosives [28], polymorphic forms of many compounds used as active pharmaceutical ingredients (API) [29, 30] in commercial medications as well as several illegal narcotic substances [31]. Since many materials are transparent to THz radiation, these items of interest can be observed through visually opaque intervening layers, such as packaging and clothing. Though not strictly a spectroscopic technique, the ultrashort width of the THz radiation pulses allows for measurements (e.g., thickness, density, location of defects) on difficult to probe materials (e.g., foam) [32, 33].

3.1. Data analysis: reflection geometry

The optical parameters of a sample may be evaluated using reflection or transmission as mentioned above. For high THz absorption media, such as fresh biological tissues, there is a limit of sample thickness for THz-TDS in transmission geometry. Over that limit, reflection geometry must be used (**Figure 3**).

Once temporal measurements are made and profiles of the sample signal and reference one are obtained, the optical parameters, such as refractive index and absorption coefficient, are then calculated. They are extracted using the following expression [34, 35].

$$\frac{E_s(\omega)}{E_{\text{ref}}(\omega)} = \frac{t_{w,s} r_{w,s}}{t_{w,s}}(\omega) \exp \left[i \frac{4\pi n_w d}{c} \right] \quad (1)$$

Where $E_s(\omega)$ is the measured electric field of the pulse reflected at the interface window-sample, $E_{\text{ref}}(\omega)$ is the measured electric field of the pulse at the front surface (air-window) of the sample holder, $r_{w,s}$ is the complex reflection coefficient for the window-sample interface to be calculated and $t_{a,w}$ and $t_{w,a}$ are, respectively, the known transmission coefficients for air-window and window-air interfaces.

Since the absorptions of the air and window are negligible (normally), the above transmission coefficients are assumed to be real; the n_w is the known refractive index of the medium used as reference (window material) and d is the effective thickness of the window, which can be calculated from

$$d = \frac{d_w}{\cos\phi} \quad (2)$$

where d_w is the thickness of the sample holder's window and ϕ is the reflection angle on the back side of the window (in contact with the sample). The known and measured quantities in Eq. (2) allow the determination of $r_{w,s}(\omega)$, which can be written in its complex form

$$r_{w,s}(\omega) = A e^{i\phi} \quad (3)$$

where A is the amplitude and ϕ is the phase. Considering the case of normal incidence, where the reflection and transmission coefficients have simpler forms, the complex reflection coefficient becomes

$$r_{w,s}(\omega) = \frac{n_w - n_s(\omega)}{n_w + n_s(\omega)} \quad (4)$$

where $n_s(\omega) = n_s + i\alpha_s(\omega)c/4\pi\nu_{\text{THz}}$ is the complex refractive index of the sample; n_s is the real part of $n_s(\omega)$, $\alpha_s(\omega)$ is the absorption coefficient; c is the speed of light in vacuum; and ν_{THz} is the frequency of THz radiation. Substituting Eq. (3) in Eq. (4), we obtain for the sample index of refraction the following expression [36]:

$$n_w(\omega) = \frac{n_w(1 - A^2)}{1 + A^2 + 2A \cos\phi} \quad (5)$$

And for absorption coefficient

$$\alpha_s(\omega) = \frac{4\pi n_s \nu}{c} \frac{-2A \sin\phi}{1 + A^2 + 2A \cos\phi} \quad (6)$$

In reflection geometry, the extraction of these frequency-dependent parameters is a bit more complicated than in transmission one, as can be seen in the following section. Similarly, for the transmission, both reference and sample signals are recorded. However, apart from a temporal shift of the sample and the reference pulse due to the reference window material, an additional spatial shift occurs due to refraction and the absorption data are contained within the phase information of the measurement, which is sensitive to system artefacts. Additionally, there is one more difficulty arising due to polarization change due to reflection under a specific angle that causes the reference and sample pulses to be differently polarized. This is relevant, since the sensitivity of the detector is polarization dependent.

4. Time-domain terahertz spectroscopy in transmission geometry

Measurement in transmission geometry (**Figure 5**), the laser beam is also split into a pump and a probe beam and so on. The signal is first enhanced by a low-noise current amplifier and then sent to the LIA, which sends reference frequency to the chopper.

A delay stage with dc-motor actuator, driven by a motion controller, moves a set of mirrors either continuously or stepwise with adjustable waiting time between steps. The mechanical

precision of the movement is typically about $0.1 \mu\text{m}$ corresponding to time shift of about 0.66 fs . In THz-TD spectrometer, three parameters are of interest: the delay stage waiting-time (t_{delay}); the LIA's time constant, the integration time (t_{LIA}); and the frequency of the chopper (ν_{chopper}). For a higher SNR and narrower amplifier bandwidth noise, longer t_{LIA} is needed [37].

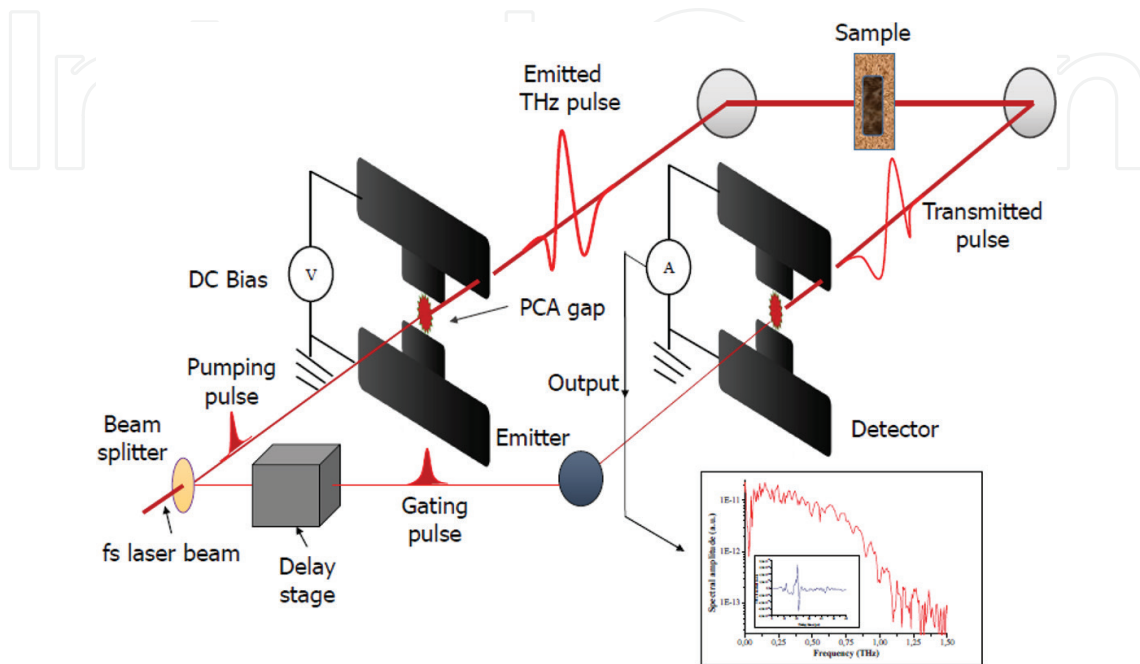


Figure 5. General experimental setup for THz-TDS in transmission geometry. The sample (colon or gastric tissue) is sandwiched in between two high density polyethylene (HDPE) or other window material sheets, normally.

4.1. Data analysis: transmission geometry

In THz-TDS measurements, the following assumptions are considered: (1) the sample under measurement is a homogeneous dielectric slab with parallel and flat surfaces, where the scattering of THz rays is negligible; (2) the incident angle of the THz beam is normal to the sample surfaces; (3) the transverse dimension of the sample is larger than the incident beam waist, so there is no diffraction; (4) the reference signal is measured under the same conditions as the sample signal; (5) the resolution of the measuring instrument is sufficiently high so that the quantization error is negligible, unless stated otherwise; (6) the measuring instruments are well calibrated; and (7) there is no human error in the measurements.

Figure 6 shows a diagram of typical sample mounting in a container (sample cell) for in transmission THz-TDS. The THz pulse propagates through a sandwich formed by two windows and an inner space containing the sample.

The determination of frequency-dependent optical constants of a sample comprehends several steps, as illustrated in **Figure 7**. Since the quantity provided by a THz-TDS measurement is a time-domain signal, then a physical model is required to relate the measured signal to the optical properties of the sample.

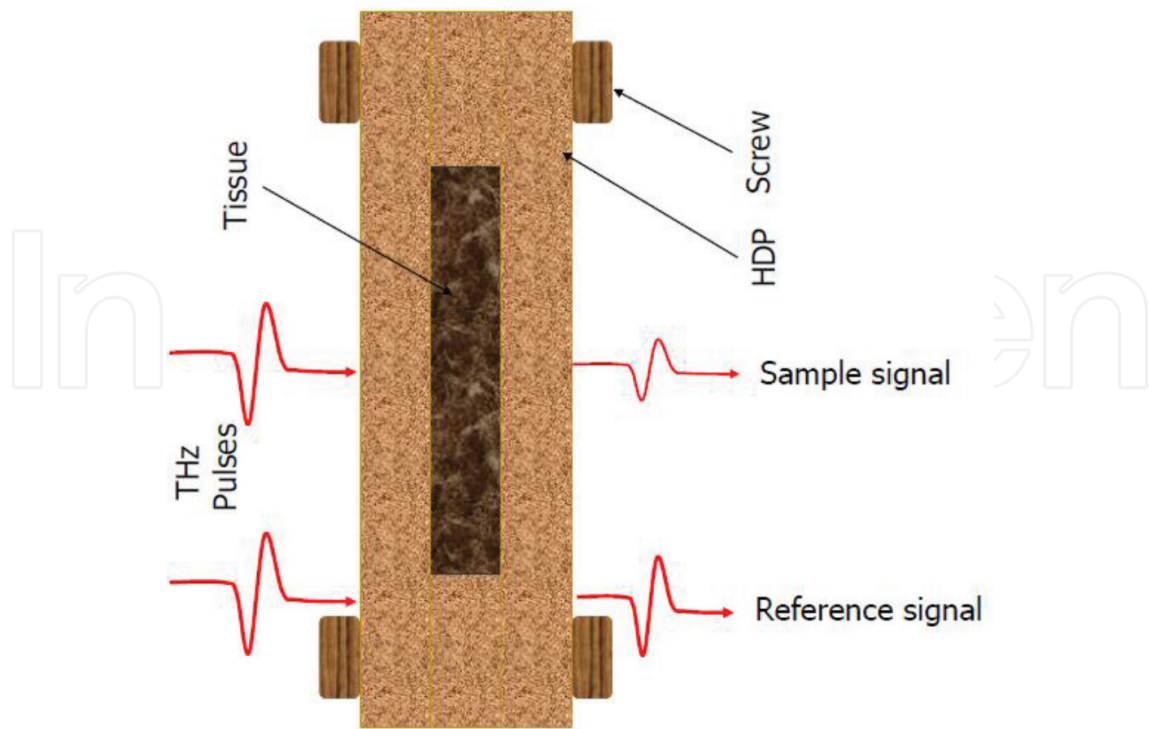


Figure 6. Sample mounting for THz-TDS in transmission geometry.

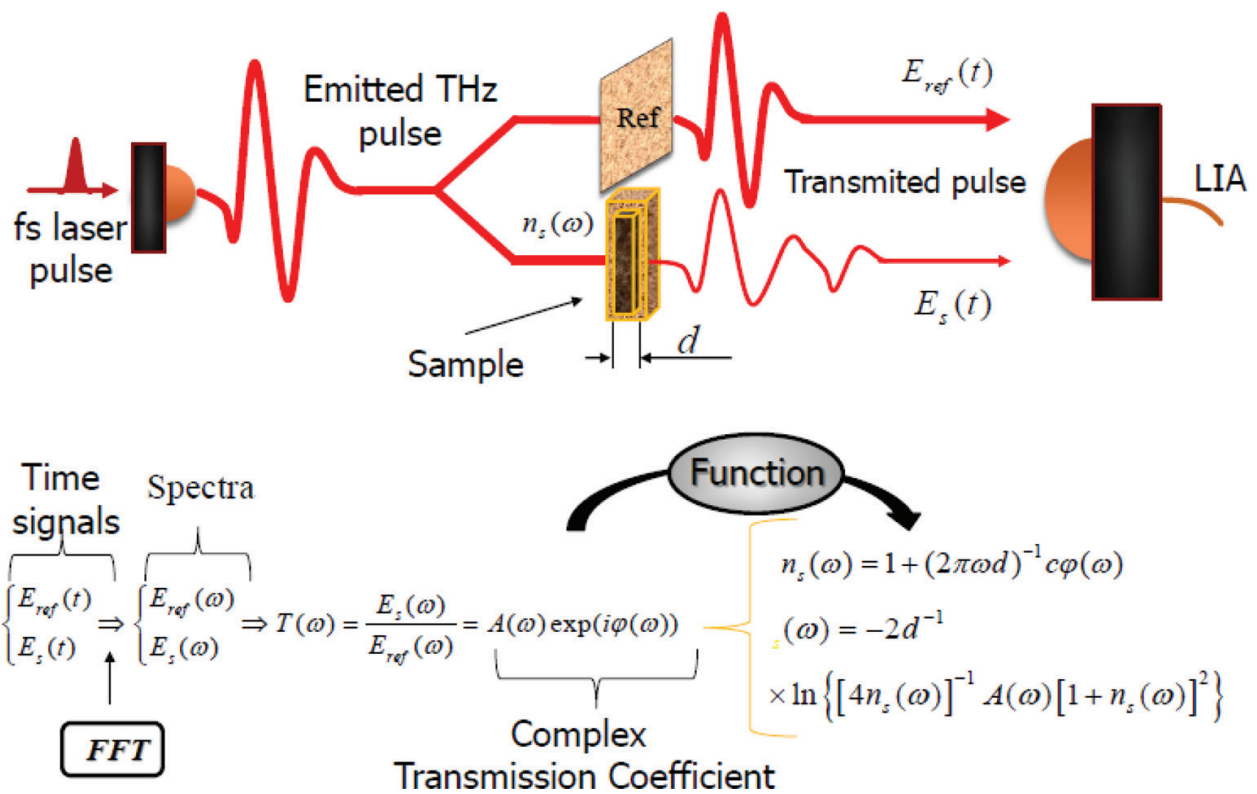


Figure 7. THz-TDS in transmission. Extraction of the real and imaginary refractive index, absorption coefficient of a sample through a fast Fourier transformation.

Normally, the waveforms of the THz pulses have very narrow time widths (~0.25 ps). As already stated, two pulses are recorded in THz-TDS: one with an empty sample holder and the other with the sample placed. The measured signal is proportional to the electric field of the THz pulse. The pulse that propagates through the sample is called sample pulse, E_s , and that propagating through the reference medium (with known dielectric constants) is the reference pulse, E_{ref} .

Knowing the time evolution of those pulses, it is possible to get the information about the frequency-dependent dielectric constants (absorption coefficient (α_s) and the refractive index (n_s) of the sample). It can be noticed that the THz signal propagates through both the reference medium and the sample, over a distance d (the thickness of the sample). **Figure 7** presents a diagram representation of a THz-TDS in transmission geometry and data processing.

The Fresnel amplitude transmission coefficients through the interfaces, reference medium-sample and sample-reference medium, are expressed, respectively, as

$$t_{M,s} = \frac{2}{M+n(\omega)} \quad \text{and} \quad t_{s,M} = \frac{2n(\omega)}{M+n(\omega)} \quad (7)$$

Where $n_s(\omega) = n_s - ik(\omega)$ is the complex refractive index of the sample. The real part of this expression denotes the refractive index of the sample and the imaginary one is related with the absorption coefficient.

Taking the Fourier transform of $E(t)$,

$$E(\omega) = \frac{1}{2\pi} \int_{-\infty}^{\infty} e^{-i\omega t} E(t) dt \quad (8)$$

The Fourier transform of the THz signal transmitted through the sample can be written as follow:

$$E_s(\omega) = E_0(\omega) t_{w,s} P h_s(\omega) t_{s,w} \quad (9)$$

Where $E_0(\omega)$ is the THz electric field shining on the first interface window-sample, $t_{w,s}$ represents the transmission coefficient of that interface, $t_{s,w}$ is the transmission coefficient of the second interface sample window and $P h_s(\omega) = e^{-i\phi_s(\omega)}$ represents the phase factor, where $\phi_s = k_s(\omega)d$ and $k_s(\omega)$ are the wave vector of the sample pulse. The phase factor represents the phase gained when the pulse propagates through the sample with thickness d .

The Fourier transform of the THz signal transmitted through the reference can be written as

$$E_{\text{ref}}(\omega) = E_0(\omega) \phi_{\text{ref}}(\omega) = E_0 e^{-i\frac{M\omega d}{c}} \quad (10)$$

Comparing with the equivalent expression for the sample signal in Eq. (9), we observe that the transmission coefficients are absent since they are equal to unit. The ratio of the two signals, $E_s(\omega)$ and E_{ref} gives the complex transmission of the sample, in some literatures, called transfer function. For normal incidence, this function can be expressed as [34]

$$T(\omega) = \frac{E_s(\omega)}{E_{\text{ref}}(\omega)} = \frac{4 n_s(\omega)}{(n_s(\omega) + M)^2} \exp \left[i \frac{\omega d}{c} (n_s(\omega) - M) \right] \quad (11)$$

The effect of multiple reflections in the interfaces, reference medium-sample and sample-reference medium (i.e., Fabry-Pérot effect [38, 39]), may be accounted for, by incorporating the factor $FP(\omega)$ as follows [40],

$$T(\omega) = \frac{E_s(\omega)}{E_{\text{ref}}(\omega)} = \frac{4 n_s(\omega)}{(n_s(\omega) + M)^2} \exp \left[i \frac{\omega d}{c} (n_s(\omega) - M) \right] FP(\omega) \quad (12)$$

where

$$FP(\omega) = \frac{1}{M - \left[\frac{n_s(\omega) - M}{n_s(\omega) + M} \exp(-2i n_s(\omega) \frac{\omega d}{c}) \right]} \quad (13)$$

This effect could be, however, neglected in case the samples to be analysed are thick enough so that the Fabry-Pérot echo is considerably retarded, therefore, easily discriminable from the main signal. The aim is at find the absorption coefficient and the real refractive index of the samples. As was stated before, the ratio between the sample and the reference signal may be expressed as [41],

$$\frac{E_s(\omega)}{E_{\text{ref}}(\omega)} = A(\omega) \exp(i\phi(\omega)) = \frac{4 n_s(\omega)}{(n_s(\omega) + M)^2} \exp \left[i \frac{\omega d}{c} (n_s(\omega) - M) - n_i i \frac{\omega d}{c} \right] \quad (14)$$

If in the experiments, THz transparent material be used as a reference medium then, $M = n_w$, where n_w represents the window's refractive index. Then for the refractive index and absorption coefficient of the sample, the following expressions can be written [42, 43]

$$n_s(\omega) = \frac{c\phi(\omega)}{2\pi v d} + n_w \quad (15)$$

and

$$\alpha_s(\omega) = \frac{2}{d} \ln \left[\frac{4 n_s(\omega)}{A (n_s(\omega) + n_w)^2} \right] \quad (16)$$

respectively.

In the process of extraction of the optical frequency-dependent parameters of materials, the dynamic range (DR) of a THz-TDS [44] is also taken in account. Due to the typical single-cycle regime of the THz pulse, the spectral amplitude is strong at low frequencies, and normally, a characteristic gradual roll-off occurs at high frequencies until the detected THz signal approaches the noise level at the experiment.

The DR of a THz-TDS setup is defined as the signal above the noise level of the spectrum. It is determined by the Fourier transformation of the measured temporal waveform (i.e., the spectrum of the THz radiation extracted from its time waveform in the scanning period, $0 - T$) above the noise level. The noise N includes the noise due to fluctuations in the THz field, $N_{\text{THz}}(t) = R(t) E_{\text{THz}}(t)$, where $T(t)$ is a dimensionless random ratio and N_{OPB} is the background noise from the detection of the THz. The background noise includes the optical probe-beam (OPB) shot noise

in the detector, which is proportional to the recorded current and all noises in the detector gathered together, such as Johnson noise, amplification noise, thermal noise, the zero-THz-field photocurrent, etc.

Analytically, the DR can be expressed by the expression [45].

$$\text{DR}(\omega) = \frac{\kappa(\omega)}{\sqrt{\frac{\delta t}{2\pi} \left(\frac{\kappa}{S}\right)^2 + \frac{T\delta t}{2\pi} \frac{1}{D^2}}} \quad (17)$$

where $\kappa(\omega) = E(\omega)/A_{\text{THz}}$ with A_{THz} representing the maximum amplitude of the THz field in time-domain is a factor dependent upon the actual waveform, δt is the temporal intervals at which the temporal waveform of the THz pulse is sampled, $S = 1/\sigma_R$ is the temporal measurement signal-to-noise ratio (SNR), T is the sampling range, $D = A/S_B$ where A represents the maximum amplitude of the THz field in time-domain, is the temporal dynamic range, and

$$\kappa = A^{-1} \sqrt{\int_{-\infty}^{\infty} |E(t)|^2 dt} \quad (18)$$

Actually, the DR limits the maximum magnitude of the absorption coefficient that could be observed along the higher frequencies. The effect of the DR may wrongly be perceived as an absorption peak in samples whose absorption rises with the rise of the frequencies, since the rise and the beginning of the rolling-off resemble a signal peak.

Thus, the maximum absorption coefficient, which can be measured reliably, corresponds to the situation where the sample signal is attenuated to a level approaching the noise level, that is, the maximum of absorption coefficient data reliable can be obtained only in the range within the DR of the experiment [44]:

$$\alpha_{\text{max}}(\omega) d = 2 \ln \left(\text{DR}(\omega) \frac{4 n_s(\omega)}{(n_s(\omega) + 1)^2} \right) \quad (19)$$

Values of α larger than α_{max} could cause the detector saturation and therefore cannot be measured.

5. Terahertz spectroscopy of colonic and gastric carcinoma

The intestine is part of the digestive system—a tube that begins at mouth, forms stomach, small intestine, the large bowel (colon and rectum) and ends with the anus. The colon and rectum are located in this gastrointestinal tract (GIT) [46] system [47]. It is made up of two main parts, the colon and the rectum, which are the lower part of the digestive tract measuring about 80–100 cm and 12–15 cm, respectively [48]. The colon absorbs large amount of water and salts from broken down food and the rectum stores the waste material until it is removed from our body through the anus.

Colon and rectum cancers are cancers starting in the colon and rectum, respectively. Since they have many features in common, they are very often called with a unique name of colorectal cancer. The colon and the rectum cancers develop slowly along several years. Before cancer development, a growth of tissue or benign tumour normally starts as a non-cancerous polyp (non-cancerous tumour) on the inner colon or rectum epithelium. With time, it becomes an adenomatous polyps or adenomas that are polyps potentially transiting into cancer stage.

The colon and rectum tracts are sections of the large intestine, a tube-like structure characterized by a wall consisting of layers such as mucosa (the inner lining layer), *muscularis mucosa* (a thin muscle layer outer limit of the mucosa), submucosa (the fibrous tissue beneath the *muscularis*), *muscularis propria* (a thick muscular layer) and subserosa and serosa (the outermost layer of connective tissue covering most of the colon but not the rectum) (**Figure 8**).

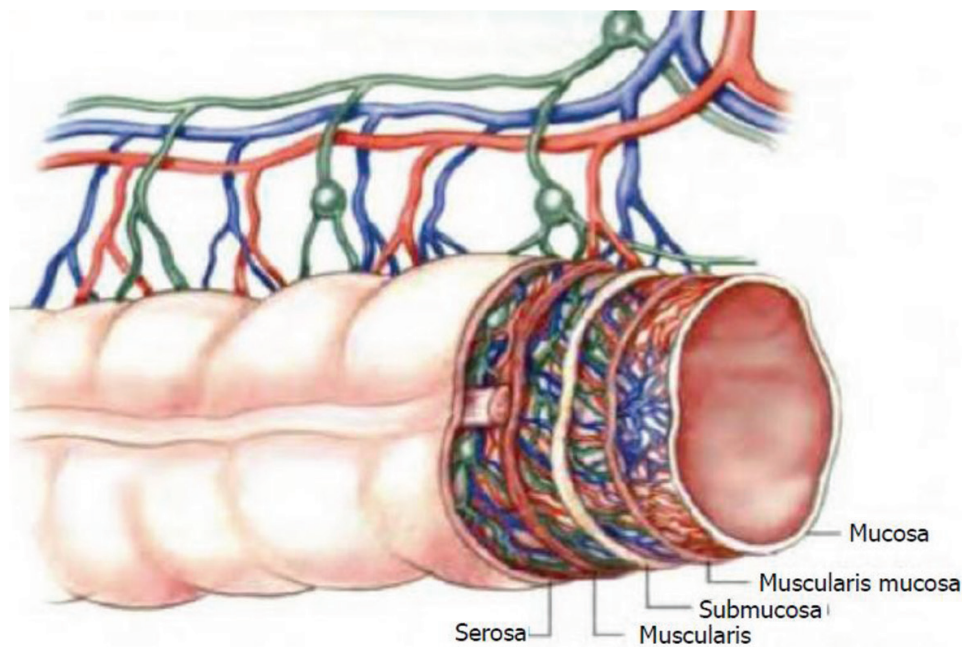


Figure 8. A section of colorectal layered wall [49].

Colon and gastric cancers are among the most commonly diagnosed cancers and death cause worldwide [50]. Early diagnosis is of utmost importance for in-time treatment. THz-TDS has demonstrated the capability to distinguish between normal and cancerous tissue as was stated and well referenced previously in this chapter. Presently, several THz-TDS systems are commercially available [51]; some of them being directly derived from laboratory set-ups, while others are compact and integrate with more sophisticated man-machine interfaces. There are, however, still many challenging issues to overcome, such as better understanding of THz wave—biological tissue interaction, which could enable the development of reliably and powerful THz diagnostic systems even for early cancer diagnosis.

6. Conclusions

Owing to the fact that THz waves have very low photon energy, that is, energy levels of few milli-electronvolt, which is well below the ionization energies of atoms and molecules [52], they do not pose any ionization hazard for biological tissues. The characteristic energies of biological media, because of molecular motions, such as rotational and vibrational ones, lie in the THz frequency band, allowing THz waves to directly detect their spectral signatures. Due to that, there is a worldwide interest in the exploitation of this frequency band and related techniques (spectroscopy and imaging) for biomedical application in the last two decades with much more terahertz spectra being reported in spectroscopic studies of cancer, particularly.

Water is essential in biological systems [53], and it plays a key role as the solvent in molecular reactions. It shows characteristic absorption features mainly the infrared (IR) and THz bands, due to which its resonance is related to symmetric stretch, bending, libration and rotation, which are modified by hydrogen bonding in the liquid state. THz waves are very sensitive to water content and strongly attenuated by water in which biological molecules reside [54–57]. The presence of cancer often causes increased blood supply to affected tissues and a local increase in tissue water content may be observed [58–60]: this fact acts as a natural contrast mechanism for terahertz spectroscopy of cancer. Furthermore, the structural changes that occur in affected tissues have also been shown to contribute to terahertz spectroscopy contrast.

The THz techniques as THz-TDS, providing broadband information on biological tissue and which make possible the discrimination of tissue regions with different optical characteristics (e.g., neoplastic and non-neoplastic tissue) over working THz frequency range, are thus expected to bring a more comprehensive screening and diagnosis of human disease, particularly in the case of cancer.

The THz transmission spectroscopy has previously been used to obtain the THz optical characteristics of skin tissue [61–63]. THz-pulsed spectroscopy has also been used to successfully characterize DNA and proteins [64, 65], allowing intermolecular interactions to be probed. The THz-TDS combined with THz imaging could be used for macroscopic visualization of tumour margins in fresh tissues according to first published results on cancer tissue imaging using THz-pulsed radiation [66], and later confirmed by studies on various cancer types and organs [67].

This chapter presents some arguments that indicate that THz-TDS has the potential [68, 69] to be a superior complement to the techniques for cancer screening in use nowadays. In the work of several groups with freshly excised tissues, the differences on the refractive indices and absorption coefficients in dysplastic tissues have been mainly attributed to the presence of a higher water content. However, other possible factors have been pointed out by authors of numerous studies [70–72]. Additional studies are needed towards the determination of all of the contrast-contributing factors other than water towards an efficient, reliable and functional THz techniques and methods. Some cancer contrast factors are already known such as (1) the increase in the vasculature due to the release of growth factors that also lead to rapid cell division and higher cell densities; (2) the conditions within the tumour microenvironment that differ considerably from those of normal tissue, for instance, low

oxygen levels (hypoxia). Angiogenesis is one of the main responses of the tumour to overcome the hypoxia; (3) the rapid and uncontrolled cell division that leads to an increased cell density and/or to the presence of certain proteins; and (4) tryptophan degradation in women with breast cancer [73], and it shows a resonance absorption peak at 1.435 THz [74], and other amino acids play a crucial role in the proliferation of tumour cells and their influence in the contrast is still in evaluation. There is a dependence of the tumour development upon the nutrients received through the blood. Tumour cells, like all other cells, need amino acids for their proliferation. The majority of the tumour cells have the capability to gather amino acids more than normal cells can [75].

In THz-TDS, the dysplastic tissue normally shows higher refractive indices and absorption coefficients that distinguish them from the normal ones. This fact could reinforce the feasibility of THz-TDS technique for gastrointestinal cancer detection. Furthermore, the works in this area demonstrate that the higher percentage of water in cancerous tissues is not the only factor contributing to the contrast of the observed through refractive indices and absorption coefficients spectra [76].

Author details

Faustino Wahaia^{1,2*}, Irmantas Kašalynas³, Gintaras Valušis³, Catia D. Carvalho Silva⁴ and Pedro L. Granja^{1,2,5,6}

*Address all correspondence to: fwahaia@fc.up.pt

1 Institute for Innovation and Health Research (i3S), University of Porto, Porto, Portugal

2 Institute of Biomedical Engineering (INEB), University of Porto, Porto, Portugal

3 Department of Optoelectronics, Center for Physical Sciences and Technology, Vilnius, Lithuania

4 Centro Hospitalar São João, Porto, Portugal

5 Institute of Biomedical Sciences Abel Salazar (ICBAS), Universidade do Porto, Porto, Portugal

6 Faculty of Engineering, University of Porto (FEUP), Porto, Portugal

References

- [1] Gallerano GP. Overview of Terahertz Radiation Sources. In: *FEL Conference*; 2004. Publ. JACoW.Org
- [2] Mukherjee P, Gupta B. Terahertz (THz) Frequency sources and antennas – a brief review. *Int J Infrared Millimeter Waves*. 2008;29(12):1091–1102. doi:10.1007/s10762-008-9423-0.
- [3] Nagatsuma T, Kaino A, Hisatake S, et al. Continuous-wave terahertz spectroscopy system based on photodiodes. *PIERS Online*. 2010;6:390–394. doi:10.2529/PIERS091029132808.

- [4] Nishizawa J, Suto K, Sasaki T, et al. Spectral measurement of terahertz vibrations of biomolecules using a GaP terahertz-wave generator with automatic scanning control. *J Phys D Appl Phys*. 2003;36(23):2958–2961. doi:10.1088/0022-3727/36/23/015.
- [5] Woodward RM, Wallace VP, Arnone DD, Linfield EH, Pepper M. Terahertz pulse imaging of skin cancer with time and frequency domain. *J Biol Phys*. 2003;29:257–261.
- [6] Ferguson B, Zhang X-C. Materials for terahertz science and technology. *Nat Mater*. 2002;1(1):26–33. doi:10.1038/nmat708.
- [7] Pickwell E, Wallace VP. Biomedical applications of terahertz technology. *J Phys D Appl Phys*. 2006;39(17):R301–R310.
- [8] Kaindl RA, Carnahan MA, Hägele D, Lövenich R, Chemla DS. Ultrafast terahertz probes of transient conducting and insulating phases in an electron-hole gas. *Nature*. 2003;423(6941):734–738. doi:10.1038/nature01676.
- [9] Seibert JA, Boone JM. X-ray imaging physics for nuclear medicine technologists. Part 2: X-ray interactions and image formation. *J Nucl Med Technol*. 2005;33(1):3–18. doi:33/1/3 [pii].
- [10] Yin X-X, Hadjiloucas S, Zhang Y. Complex extreme learning machine applications in terahertz pulsed signals feature sets. DOI: <http://dx.doi.org/10.1016/j.cmpb.2014.06.002>
- [11] Fan S, He Y, Ung BS, et al. The growth of biomedical terahertz research. *J Phys D Appl Phys*. 2014;47(37):374009. doi:10.1088/0022-3727/47/37/374009.
- [12] Globus T. Sub-terahertz vibrational spectroscopy with high resolution for biological molecules and cells identification. *J Biomol Res Ther*. 2016;2016. doi:10.4172/2167-7956.1000E150.
- [13] Yang X, Zhao X, Yang K, et al. Biomedical applications of terahertz spectroscopy and imaging. *Trends Biotechnol*. 2016;34(10):810–824. doi:10.1016/j.tibtech.2016.04.008.
- [14] Schirmer M, Fujio M, Minami M, Miura J, Araki T, Yasui T. Biomedical applications of a real-time terahertz color scanner. *Biomed Opt Express*. 2010;1(2):354–366. doi:10.1364/BOE.1.000354.
- [15] Fischer BM, Helm H, Jepsen PU. Chemical recognition with broadband THz spectroscopy. *Proc IEEE*. 2007;95(8):1592–1604. doi:10.1109/JPROC.2007.898904.
- [16] Kimmit MF. Restrahlen to T-rays—100 years of terahertz radiation. *J Biol Phys*. 2003;29:75–85.
- [17] Tonouchi M. Cutting-edge terahertz technology. *Nat Photonics*. 2007;1(2):97–105. doi:10.1038/nphoton.2007.3.
- [18] Uhd JP, Jacobsen RH, Keiding SR. Generation and detection of terahertz pulses from biased semiconductor antennas. *Journal of the Optical Society of America B*. 1996;13(11):2424–2436.
- [19] Wahaia F, Valusis G, Bernardo LM, et al. Detection of colon cancer by terahertz techniques. *J Mol Struct*. 2011;1006(1–3):77–82. doi:10.1016/j.molstruc.2011.05.049.

- [20] Rolf Hulthén. Kramers–Kronig relations generalized: on dispersion relations for finite frequency intervals. A spectrum-restoring filter. *Journal of the Optical Society of America*. 1982;72(6):794–803.
- [21] Mickan SP, Lee K-S, Lu T-M, Munch J, Abbott D, Zhang X-C. Double modulated differential THz-TDS for thin film dielectric characterization. *Microelectronics Journal*. 33 (2002) 1033–1042.
- [22] Chen Y, Liu H, Deng Y, et al. THz spectroscopic investigation of 2,4-dinitrotoluene. *Chem Phys Lett*. 2004;400(4-6):357–361. doi:10.1016/j.cplett.2004.10.117.
- [23] Un-ichi Shikata, Hiroyuki Handa et al. Terahertz ATR spectroscopy of liquids using THz-wave parametric sources. 2007 Conf Lasers Electro-Optics, IEEE - Pacific Rim. 2007:1–2.
- [24] Hirori H, Yamashita K, Nagai M, et al. Attenuated total reflection spectroscopy in time domain using terahertz coherent pulses. *Jpn J Appl Phys*. 2004;43(No. 10A):L1287–L1289. doi:10.1143/JJAP.43.L1287.
- [25] Nagai M, Yada H, Arikawa T, Tanaka K. Terahertz time-domain attenuated total reflection spectroscopy in water and biological solution. *Int J Infrared Millimeter Waves*. 2007;27(4):505–515. doi:10.1007/s10762-006-9098-3.
- [26] Hindle F, Yang C, Mouret G, et al. Recent developments of an opto-electronic THz spectrometer for high-resolution spectroscopy. *Sensors (Basel)*. 2009;9(11):9039–9057. doi:10.3390/s91109039.
- [27] Schubert O, Hohenleutner M, Langer F, et al. Sub-cycle control of terahertz high-harmonic generation by dynamical Bloch oscillations. *Nature Photonics*. 2014;8:119–123.
- [28] Liu H-B, Zhang X-C. Terahertz Spectroscopy for Explosive, Pharmaceutical, and Biological Sensing Applications. In: *Terahertz Frequency Detection and Identification of Materials and Objects*. Dordrecht:Springer Netherlands;2007:251–323. doi:10.1007/978-1-4020-6503-3_17.
- [29] Kissi EO, Bawuah P, Silfsten P, Peiponen K-E. A tape method for fast characterization and identification of active pharmaceutical ingredients in the 2–18 THz spectral range. *J Infrared, Millimeter, Terahertz Waves*. 2015;36(3):278–290. doi:10.1007/s10762-014-0123-7.
- [30] Larkin PJ, Dabros M, Sarsfield B, Chan E, Carriere JT, Smith BC. Polymorph characterization of active pharmaceutical ingredients (APIs) using low-frequency Raman spectroscopy. *Appl Spectrosc*. 2014;68(7):758–776. doi:10.1366/13-07329.
- [31] Dobroiu A, Sasaki Y, Shibuya T, Otani C, Kawase K. THz-wave spectroscopy applied to the detection of illicit drugs in mail. *Proc IEEE*. 2007;95(8):1566–1575. doi:10.1109/JPROC.2007.898840.
- [32] Abina A, Puc U, Jeglič A, Zidanšek A. Applications of terahertz spectroscopy in the field of construction and building materials. *Appl Spectrosc Rev*. 2015;50(4):279–303. doi:10.1080/05704928.2014.965825.

- [33] Mangeney J. THz photoconductive antennas made from ion-bombarded semiconductors. *J Infrared, Millimeter, Terahertz Waves*. 2012;33(4):455–473. doi:10.1007/s10762-011-9848-8.
- [34] Duvillaret L, Garet F, Coutaz J-L. A reliable method for extraction of material parameters in terahertz time-domain spectroscopy. *IEEE J Sel Top Quantum Electron*. 1996;2(3):739–746. doi:10.1109/2944.571775.
- [35] Krüger M, Funkner S, Bründermann E, Havenith M. Uncertainty and ambiguity in terahertz parameter extraction and data analysis. <http://dx.doi.org/10.1007/>. Accessed October 23, 2016.
- [36] Obradovic J, Collins JHP, Hirsch O, Mantle MD, Johns ML, Gladden LF. The use of THz time-domain reflection measurements to investigate solvent diffusion in polymers. *Polymer (Guildf)*. 2007;48(12):3494–3503. doi:10.1016/j.polymer.2007.04.010.
- [37] Mickan SP, Lee K-S, Lu T-M, et al. Thin film characterization using terahertz differential time-domain spectroscopy and double modulation Proceedings of SPIE Vol. 4591 (2001) © 2001 SPIE · 0277-786X/01/\$15.
- [38] Dorney TD, Baraniuk RG, Mittleman DM. Material parameter estimation with terahertz time-domain spectroscopy. *J Opt Soc Am A*. 2001;18(7):1562. doi:10.1364/JOSAA.18.001562.
- [39] Scheller M. Data extraction from terahertz time domain spectroscopy measurements. *J Infrared, Millimeter, Terahertz Waves*. 2014;35(8):638–648. doi:10.1007/s10762-014-0053-4.
- [40] Lee JW, Seo MA, Kim DS, et al. Fabry–Perot effects in THz time-domain spectroscopy of plasmonic band-gap structures. *Appl Phys Lett*. 2006;88(7):71114. doi:10.1063/1.2174104.
- [41] Duvillaret L, Garet F, Coutaz J-L. A reliable method for extraction of material parameters in terahertz time-domain spectroscopy. *IEEE J Sel Top Quantum Electron*. 1996;2(3):739–746
- [42] He M, Li M, Zhang W. Terahertz time-domain spectroscopy signature of animal tissues. 2008:274–277.
- [43] Ying H, Huang P, Guo L, Wang, Zhang C. Terahertz spectroscopic investigations of explosives. *Phys Lett*. 2006;359:728–732.
- [44] Jepsen PU, Fischer BM. Dynamic range in terahertz time-domain transmission and reflection spectroscopy. *Opt Lett*. 2005;30(1):29–31.
- [45] Xu J, Yuan T, Mickan S, Zhang X-C. Limit of spectral resolution in terahertz time-domain spectroscopy. *Chines Phys Lett*. 2003;20(8):1266–1268.
- [46] Gremel G, Wanders A, Cedernaes J, et al. The human gastrointestinal tract-specific transcriptome and proteome as defined by RNA sequencing and antibody-based profiling. *J Gastroenterol*. 2015;50(1):46–57. doi:10.1007/s00535-014-0958-7.
- [47] B. ODE, J.C. Alcohol and the gastrointestinal tract. *Advances in Internal Medicine and Pediatrics*. 1980;45:1–75.

- [48] Camilleri M, Linden DR. Measurement of gastrointestinal and colonic motor functions in humans and animals. *C Cell Mol Gastroenterol Hepatol*. 2016;2(4):412–428. doi:10.1016/j.jcmgh.2016.04.003.
- [49] NCI. The Cancer of the Colon and Rectum. (Institute NC, ed.). NIH; 2006. ISBN: 0-309-65952-3, 340 pages, 6 x 9, (2006).
- [50] Fitzmaurice C, Dicker D, Pain A, et al. The global burden of cancer 2013. *JAMA Oncol*. 2015;1(4):505. doi:10.1001/jamaoncol.2015.0735.
- [51] Hochrein T. Markets, availability, notice, and technical performance of terahertz systems: Historic development, present, and trends. *J Infrared, Millimeter, Terahertz Waves*. 2015;36(3):235–254. doi:10.1007/s10762-014-0124-6.
- [52] Ionization and Fragmentation of Complex Molecules and Clusters. Henrik A. B. Johansson, Stockholm 2011. ISBN 978-91-7447-399-5.
- [53] Png GM, Choi JW, Ng B, Mickan SP, Abbott D. The impact of hydration changes in fresh bio-tissue on THz spectroscopic measurements. *Phys Med Biol*. 2008;53:3501–3517.
- [54] Wahaia F, Valusis G, Bernardo LM, et al. Detection of colon cancer by terahertz techniques. *J Mol Struct*. 2011;1006(1–3):77–82. doi:10.1016/j.molstruc.2011.05.049.
- [55] Wallace VP, Fitzgerald AJ, MacPherson EP, Taday RJPFF, Flanagan N, Ha T. Terahertz pulsed spectroscopy of human basal cell carcinoma. *Appl Spectrosc*. 2006;60(10):1127–1133.
- [56] MacPherson EP, Fitzgerald AJ, Taday PF, et al. Terahertz imaging and spectroscopy of skin cancer. *Biol Med Appl*. 2004:821–822.
- [57] Sun Y, Fischer MB, MacPherson EP. Effects of formalin fixing on the THz properties of biological tissues. *J Biol Opt*. 2009;14(6):6401–6417.
- [58] Reynolds TY, Rockwell S, Glazer PM. Genetic instability induced by the tumor microenvironment. *Cancer Res*. 1996;56:5754–5757.
- [59] McIntyre GI. Cell hydration as the primary factor in carcinogenesis: Unifying concept. *Med hypothesis*. 2006;66:518–526.
- [60] McIntyre GI. Increased cell hydration promotes both tumor growth and metastasis: A biochemical mechanism consistent with genetic signatures. *Med hypothesis*. 2007;69:1127–1130.
- [61] Ashworth PC, Pickwell-MacPherson E, Provenzano E, et al. Terahertz pulsed spectroscopy of freshly excised human breast cancer. *Opt Express*. 2009;15:12444.
- [62] Pickwell E, Cole B, Fitzgerald AJ, Pepper M, vivo study of human skin using pulsed terahertz radiation Phys. in Med. VPW 2004 I, 1595-1607 B 49. In vivo study of human skin using pulsed terahertz radiation. *Phys Med Biol*. 2004;49:1595–1607.
- [63] Fitzgerald AJ, Berry E, Zinov'ev NN, et al. Catalogue of human tissue optical properties at terahertz frequencies. *J. Biol. Phys*. 2003;29(2–3):123–128.

- [64] Tatiana Globus, Tatyana Khromova et al., Terahertz characterization of dilute solutions of DNA. Proc. SPIE 6093, Biomedical Vibrational Spectroscopy III: Advances in Research and Industry, 609308 (2006).
- [65] Xu J, Plaxco KW, Allen SJ. Probing the collective vibrational dynamics of a protein in liquid water by terahertz absorption spectroscopy. *Protein Sci.* 2006;15(5):1175–1181. doi:10.1110/ps.062073506.
- [66] Wallace VP, Fitzgerald AJ, Pickwell E, Pye RJ, Taday PF, Flanagan N and Ha T. Terahertz pulsed spectroscopy of human basal cell carcinoma. *Appl Spectrosc.* 2006;60(10):1127–1133.
- [67] Brun M-A, Formanek F, Yasuda A, Sekine M, Ando N, Eishii Y. Terahertz imaging applied to cancer diagnosis. *Phys Med Biol.* 2010;55(16):4615–4623. doi:10.1088/0031-9155/55/16/001.
- [68] Yu C, Fan S, Sun Y, Pickwell-Macpherson E. The potential of terahertz imaging for cancer diagnosis: A review of investigations to date. *Quant Imaging Med Surg.* 2012;2(1):33–45. doi:10.3978/j.issn.2223-4292.2012.01.04.
- [69] Doradla P, Alavi K, Joseph C, Giles R. Detection of colon cancer by continuous-wave terahertz polarization imaging technique. *J Biomed Opt.* 2013;18(9):90504. doi:10.1117/1.JBO.18.9.090504.
- [70] Chung SH, Cerussi AE, Klifa C, et al. In-vivo water state measurements in breast cancer using broadband diffuse optical spectroscopy. *Phys Med Biol.* 2008;53:6713–6727.
- [71] Wahaia F. Spectroscopic and imaging techniques using terahertz frequency band for biomedical applications. PhD Thesis (2011).
- [72] Ashworth PC, Pickwell-MacPherson E, Pinder SE, et al. Terahertz spectroscopy of breast tumors. In: *Infrared and Millimeter Waves, 2007 and the 2007 15th International Conference on Terahertz Electronics. IRMMW-THz. Joint 32nd International Conference on;* 2007:603–605.
- [73] Lyon DE, Walter JM, Starkweather AR, Schubert CM, McCain NL. Tryptophan degradation in women with breast cancer: A pilot study. *BMC Res Notes.* 2011;4:156. doi:10.1186/1756-0500-4-156.
- [74] Yu B, Zeng F, Xing YYQ, et al. Torsional vibrational modes of tryptophan studied by terahertz time-domain spectroscopy. *Biophys J.* 2004;86:1649–1654.
- [75] Cherkasova OP, Nazarov MM, Shkurinov AP. Terahertz spectroscopy of biological molecules. *Radiophys Quantum Electron.* 2009;52 (7):518–523.
- [76] Wahaia F, Kasalynas I, Seliuta D, et al. Study of paraffin-embedded colon cancer tissue using terahertz spectroscopy. *J Mol Struct.* 2015;1079:448–453. doi:10.1016/j.molstruc.2014.09.024.